Analysis of Weak and Strong Fiber Bragg Grating

Mohamed B. El-Mashade[1*], A. E. Abdelnaiem[2], W. S. El-Deeb[2] and N. I. Tawfik[3]

[1]*Department of Electrical Engineering, Faculty of Engineering, Al-Azhar University, Nasr City, Cairo, Egypt.*
[2]*Faculty of Engineering, Zagazig University, Egypt.*
[3]*Higher Technological Institute, 10th of Ramadan City, Egypt.*

Authors' contributions

This work was carried out in collaboration between all authors. All authors read and approved the final manuscript.

Original Research Article

ABSTRACT

Because of the importance of fiber Bragg grating in designing new devices to meet a need range of optical communication systems, it has attracted a great deal of attention. Fiber Bragg gratings have become a key technology in many applications. They are widely used in optical communication systems as a narrow band filters, dispersion compensators, fiber's sensors and dense wavelength division multiplexing. Advanced functionalities of fiber Bragg grating can be achieved by controlling its structural parameters. This paper is devoted to the modeling and simulation of weak and strong fiber Bragg gratings. The simulation is based on the solution of the coupled mode equations. The effect of the structural parameters such as grating length, refractive index modulation and grating period on the reflectivity, spectral bandwidth and maximum wavelength is studied. Additionally, the role of a new parameter, which is known as fringe visibility, that it can play in controlling the spectral response of the grating is also investigated. The results show that the reflectivity increases by increasing the grating length, refractive index modulation, or fringe visibility and will be decreased by

_____

Corresponding author: E-mail: ElMashade@Yahoo.Com;

increasing the grating period. Additionally, the influence of the spectral bandwidth and maximum wavelength by the changing of the grating's parameters is also taken into account in studying the two types of fiber grating.

1. INTRODUCTION

Owing to the ever-increasing need for communication capacity, the field of optics has brought into focus for the past decades. On the parallel fashion, the dramatic reduction of transmission loss in optical fibers coupled with equally important developments in the area of light sources and detectors have brought about a phenomenal growth of the fiber optic industry during the past two decades. Its high bandwidth capabilities and low attenuation characteristics make it ideal for gigabit data transmission and beyond. The birth of optical fiber communication coincided with the fabrication of low-loss optical fibers and room-temperature operation of semiconductor lasers in 1970. Optical fibers have revolutionized the modern telecommunication industry. Much of its success lies in its near-ideal properties: low transmission loss, high optical damage threshold, and low optical nonlinearity. Due to these merits, optical fiber communication technology has been deployed widely all over the world and has become an integral part of telecommunications. On the other hand, optical fibers offer a much higher capacity, a smaller size, a lesser weight, as well as it has an immunity to electromagnetic interference effects, in comparison with copper cables. Therefore, it is beneficial to use it as a communication medium instead of other competing media. This is actually the case for modern communication systems where the optical fiber gradually replaces copper cables. As a consequence of this situation, it will become necessary for many of the electronic network components to be replaced by equivalent optical components. Consequently, for all such optical components to be economical, compatible, easily manufactured, and comfortably integrated, it is of importance to use optical fiber in their fabrication [1-5].

Fiber optic photosensitivity has indeed opened a new era in the field of fiber optic based devices. Photosensitivity refers to a permanent change in the index of refraction of the fiber core when exposed to light with characteristic wavelength and intensity that depend on the core material. It has the ability to alter the core index of refraction in a single-mode optical fiber through the optical absorption of UV light. The photosensitivity of optical fibers allows the fabrication of phase structures directly into the fiber core, called fiber Bragg gratings (FBGs). A grating, on the other hand, is a device that periodically modifies the phase or the intensity of a wave reflected on, or transmitted through, it. The uniform means that the grating period "Λ" and the refractive index change "δn" are constant over the whole length of the grating. The operation of FBGs is based on the principle of Bragg reflection. When light propagates by periodically alternating regions of higher and lower refractive index, it is partially reflected at each interface between those regions. If the spacing between such specified regions is such that all the partial reflections add up in phase; when the round trip of the light between the two reflections is an integral number of wavelengths; the total reflection can grow to nearly cent percent, even if the individual reflections are very small. Of course, that condition will only hold for specific wavelengths. For all other wavelengths, the out-of-phase reflections end up cancelling each other, resulting in high transmission. Based on this principle of operation, the FBG represents a key element in fiber components [6-9].

Recently, optical FBGs have attracted a great deal of attention because of their importance in designing new devices to meet a need range of optical communication systems. An intense investigation of the possibility of using this device for all optical ultrafast applications is achieved by allowing its dielectric characteristics to be varied in such a way that a periodic perturbation of its refractive index along its optical length will be formed. The inline optical fiber based component demonstrated the tremendous potential applications over the optical components fabricated through the lithographic techniques. On the other hand, FBG is an optical wavelength filter created by the periodic modulation of the refractive index of the optical fiber's core. This modulation can be achieved mechanically or electrically. Mechanical modulation can be carried out by the variation of the core diameter, whilst electrical modulation was obtained by varying the

refractive index of the core along the fiber length. At each change of the refractive index, a reflection of the propagating light occurs. The repeated modulation of the refractive index results in multiple reflections of the forward travelling light. The period of index modulation relative to the wavelength of the light determines the relative phase of all the reflected signals. At a particular wavelength, all reflected signals are in phase and add constructively and a back reflected signal centered about the Bragg wavelength is observed. The reflected contributions from light at other wavelengths do not add constructively and are cancelled out so that these wavelengths are transmitted through the grating. Fiber Bragg gratings are most commonly used as wavelength selective reflectors and dispersion compensators in optical communication systems. Most common applications of fiber Bragg grating include: wavelength division multiplexing systems, Raman amplifiers, dispersion compensators, and CDMA systems.

Normally, a germanium doped silica fiber was used for the fabrication of fiber Bragg grating owing to its photosensitivity, which means that the change of the refractive index of the core is obtained by exposing it to the ultraviolet light. The amount of change of the refractive index depends on the intensity of the incident light and the duration of the exposure as well as the photosensitivity of the fiber. For improving the reflectivity of the fiber Bragg grating, the level of doping with germanium needs to be high. Pre-soaking the fiber in hydrogen, on the other hand, constitutes another technique of fabrication of FBG. This process is called hydrogenation. The most important characteristic of FBG is its flexibility in achieving the desired spectral characteristics.

The design of fiber Bragg grating depends on various parameters e.g. length of the grating, period of gratings, refractive index of core and cladding, mode of excitation conditions and temperature. Although the FBG is analyzed in literature [e.g. 1,7] for several profiles of the induced index change along the fiber axis, the optimum values of its interesting parameters, especially the fringe visibility, for the most widely used version (uniform), where the induced index is weakly or strongly changed, are not yet achieved. On the other hand, to meet the increasing demand for large capacity of the next generation of optical communication systems, there is an important need for numerically searching the optimum values of the more effective parameters, such as of fringe visibility, grating period, refractive index modulation, and grating length, that have a heavy weight on its performance. This is the motivation of this paper. These optimum parameter's values are obtained through the using of more efficient numerical methods in solving the resulting equations of the coupled mode theory. Here, we are interested in studying the spectral characteristics of two types of fiber Bragg grating: the strong and the weak FBG. The spectral characteristics of these two types are analyzed and modeled by the most widely used theory which is the coupled mode theory. Additionally, our goal is to design an FBG with maximum reflectivity and narrow bandwidth through the variation of the grating's parameters in such a way that the optimum of their values is attained. Moreover, the effect of grating period, refractive index modulation, grating length and fringe visibility on the reflectivity, spectral bandwidth and maximum wavelength is studied for the selected types of FBG. The remainder of this paper is organized as follows: section II explains the basic theory of fiber Bragg grating and its application for the underlined types. Section III deals with the simulation results obtained for both weak and strong gratings while section IV resumes our concluded remarks.

2. THEORY OF FIBER BRAGG GRATING

2.1 Coupled-mode Theory

The term grating is used to describe almost any device whose operation involves interference among multiple optical signals originating from the same source but with different relative phase shifts. Bragg gratings are widely used in fiber optic communication systems. In general, any periodic perturbation in the propagating medium serves as a Bragg grating. This perturbation is usually a periodic variation of the refractive index of the medium. Fiber gratings are attractive devices that can be used for a variety of applications, including filtering, add/drop functions, and compensating for accumulated dispersion in the system. Being all-fiber devices, their main advantages are their low loss, ease of coupling (with other fibers), polarization insensitivity, low temperature-coefficient, and simple packaging. As a result, they can be extremely low-cost devices [10].

Wave propagation in an optical waveguide is analyzed through the solution of Maxwell's equations constrained to appropriate boundary

conditions. The problem of finding solutions to the resulting wave-propagation equations is simplified by assuming weak guidance, which allows the decomposition of the modes into an orthogonal set of transversely polarized modes. The solutions provide the basic field distributions of the bound and radiation modes of the waveguide. These modes propagate without coupling in the absence of any perturbation. Coupling of specific propagating modes can occur if the waveguide has a phase and/or amplitude perturbation that is periodic with a perturbation phase/amplitude-constant close to the sum or difference between the propagation constants of the modes. The technique of coupled-mode theory is normally applied for solving this type of practical problems. The method assumes that the mode fields of the unperturbed waveguide remain unchanged in the presence of weak perturbation. This approach provides a set of first-order differential equations for the change in the amplitude of the fields along the fiber, which have analytical solutions for uniform sinusoidal periodic perturbations. In other words, the coupled mode theory is a powerful mathematical tool in analyzing the wave propagation and interactions with materials in optical waveguide. Since the fiber Bragg grating is one of the weakly guiding structures, the underlined theory can be used to analyze its optical behavior [11].

In the case of fiber grating, coupled mode theory considers the grating structure as the perturbation to an optical waveguide where coupling of guided modes occurs due to this perturbation. This theory has the advantage that it is relatively straightforward, intuitive and for most practical fiber gratings of interest it is accurate. It is used to describe the relation between structural parameters of the FBG and its spectral response. The basic idea of the considered theory is that the electric field of the waveguide with a perturbation can be represented as a linear combination of the modes that belong to the field distribution in the absence of perturbation [4]. The modal fields of the fiber can be formulated as:

$$E_{\pm j}(x, y, z) = e_{\pm jt}(x, y) \exp\left(\pm i\beta_j z\right) and \quad j = 1, 2, 3, \ldots\ldots\ldots\ldots \tag{1}$$

In the above expression, $e_{\pm jt}(x, y)$ denotes the amplitude of the transverse electric field of the jth propagating mode, "$\pm$" represents the propagation direction and β_j symbolizes the propagation constant or eigenvalue of the jth mode. The propagation of light along the optical waveguide can be described by Maxwell's equations. In terms of the coupled-mode theory, the transverse component of the electric field at position z in the perturbed fiber can be described by a linear combination of the ideal guided modes of an unperturbed fiber. In other words, the electric field transversal component can be written as:

$$\vec{E}_t(x, y, z, t) \quad = \quad \sum_k \vec{E}_k(x, y, z, t) \ + \ \vec{E}_{-k}(x, y, z, t) \tag{2}$$

By substituting the modal field representation into the above formula, the electric field takes the form:

$$\vec{E}_t(x, y, z, t) = \sum_j [A_j^+(z)\exp\left(i\beta_j z\right) + A_j^-(z)\exp\left(-i\beta_j z\right)]\vec{e}_{jt}(x, y)\exp\left(-i\omega t\right) \tag{3}$$

$A_j^+(z)$ and $A_j^-(z)$ are slowly varying amplitudes of the jth forward and backward travelling waves, respectively.

In the fiber Bragg grating, on the other hand, the index of the grating has z-dependent component along the fiber. Thus, it can be expressed as:

$$n(x, y, z) = n(z) = n_0 + \delta n_0 + \delta n(z) \cos\left[\frac{2\pi}{\Lambda}z + \emptyset(z)\right] \tag{4}$$

n_0 denotes the refractive index of the core without the perturbation, δn_0 represents the average index modulation (DC change), $\delta n(z)$ symbolizes the small amplitude of the index modulation (AC change), $\emptyset(z)$ is the phase of the grating, and Λ indicates the grating period. Under the weak propagation approximation, the distribution of the propagating electric field in the grating satisfies the scalar wave equation.

This follows from the simplification of Maxwell's equations which leads to:

$$[\nabla_t^2 + k^2 n^2(x,y,z) - \beta^2] \, \vec{E}_t(x,y,z,t) = 0 \tag{5}$$

Where k denotes the free space wave number (k=2π/λ) and λ symbolizes the free space wavelength. The substitution of the electric field $\vec{E}_t(x,y,z,t)$ and the refractive index $n(x,y,z)$ into the wave propagation equation yields the following coupled-mode equations:

$$\frac{dA_n^+}{dz} = i \sum_m A_m^+ \left(K_{mn} + \overline{K}_{mn}\right) \exp[i(\beta_m - \beta_n)z] + i \sum_m A_m^- \left(K_{mn} - \overline{K}_{mn}\right) \exp[-i(\beta_m + \beta_n)z] \tag{6}$$

and

$$\frac{dA_n^-}{dz} = -i \sum_m A_m^+ \left(K_{mn} - \overline{K}_{mn}\right) \exp[i(\beta_m + \beta_n)z] - i \sum_m A_m^- \left(K_{mn} + \overline{K}_{mn}\right) \exp[-i(\beta_m - \beta_n)z] \tag{7}$$

In the above formulas, $K_{mn}(z)$ represents the transverse coupling coefficient between modes m and n. This coefficient has a form given by:

$$K_{mn}(z) = \frac{\omega}{4} \iint \Delta\varepsilon(x,y,z) \, e_{mt}(x,y) \, e_{nt}^*(x,y) \; dx \; dy \tag{8}$$

$\Delta\varepsilon$ denotes the perturbation of the permittivity. In the case where the waveguide is weak, i. e. $n \gg \delta n$, $\Delta\varepsilon = 2n\delta n$. In that case, the longitudinal coefficient $\overline{K}_{mn}$ is smaller than the transversal coefficient $K_{mn}(z)$ and therefore, it can be neglected. If we assume that there are no waves propagating in the cladding of the single mode fiber, only basic counter-propagating modes exist in the fiber. Under the two-mode approximation, the coupled mode equations of Bragg gratings can be simplified to become:

$$\frac{dR(z)}{dz} = i\hat{\sigma}(z) \, R(z) \; + \; ik(z) \, S(z) \tag{9}$$

and

$$\frac{dS(z)}{dz} = -i\hat{\sigma}(z) \, S(z) \; - \; ik^*(z) \, R(z) \tag{10}$$

with

$$R(z) = A^+(z) \, \exp\left[i \left(\delta z - \frac{\varphi}{2}\right)\right] \qquad \& \qquad S(z) = A^-(z) \, \exp\left[-i \left(\delta z + \frac{\varphi}{2}\right)\right] \tag{11}$$

$R(z)$ & $S(z)$ denote the forward reverse modes, respectively, and the two types of modes are slowly varying mode envelope functions. $\hat{\sigma}$ represents a general "DC" self-coupling coefficient, also called local detuning; and $k(z)$ stands for the "AC" coupling coefficient, also called local grating strength. Mathematically, the general "DC" coupling coefficient can be formulated as:

$$\hat{\sigma} = \delta + \sigma - \frac{1}{2} \frac{d\varphi}{dz} \tag{12}$$

The last term in the above expression describes the possible chirp of the grating period. Furthermore, the detuning δ depends upon the propagation constant and the grating period according to:

$$\delta = \beta - \frac{\pi}{\Lambda} = \beta - \beta_D = 2\pi n_{eff}\left(\frac{1}{\lambda} - \frac{1}{\lambda_D}\right) \qquad \& \qquad \lambda_D \triangleq 2 \, n_{eff} \, \Lambda \tag{13}$$

λ_D refers to the design wavelength. The "DC" coupling coefficient, on the other hand, is given by:

$$\sigma \quad \triangleq \quad \frac{2\pi}{\lambda} \quad \overline{\delta n}_{eff} \tag{14}$$

$\overline{\delta n}_{eff}$ denotes the averaging of the background refractive index change. The "AC" coupling coefficient $k(z)$ can be mathematically modeled as:

$$k(z) \quad \triangleq \quad \frac{\pi}{\lambda} \quad \delta n(z) \quad g(z) \quad v \tag{15}$$

Where $g(z)$ refers to the function of the apodization, and v denotes the fringe visibility. The reflection and transmission coefficients can be evaluated through the coupled-mode equations and the initial conditions which can be summarized as follows: when there is no input signal incident from the right hand side of the grating so $S(+L/2) = 0$, there is some known signal that is incident from the left side of the grating which means that $R(-L/2) = 1$. Under these assumptions, the amplitude of the reflection coefficient can be written as:

$$\rho \quad \triangleq \quad S\left(-\frac{L}{2}\right) \bigg/ R\left(-\frac{L}{2}\right) \tag{16}$$

In terms of ρ, the power reflection coefficient (reflectivity) can be formulated as:

$$r \quad \triangleq \quad |\rho^2| \tag{17}$$

The solution of the coupled-mode equations for uniform fiber Bragg grating will lead to the calculation of the amplitude and power reflection coefficients which have mathematical forms given by [5]:

$$\rho \quad = \quad \frac{-k \sinh\left(\sqrt{k^2 - \hat{\sigma}^2}\, L\,\right)}{\hat{\sigma} \sinh\left(\sqrt{k^2 - \hat{\sigma}^2}\, L\,\right) + i\sqrt{k^2 - \hat{\sigma}^2} \cosh\left(\sqrt{k^2 - \hat{\sigma}^2}\, L\right)} \tag{18}$$

and

$$r \quad = \quad \frac{sinh^2\left(\sqrt{k^2 - \hat{\sigma}^2}\, L\,\right)}{cosh^2\left(\sqrt{k^2 - \hat{\sigma}^2}\, L\,\right) - \frac{\hat{\sigma}^2}{k^2}} \tag{19}$$

At resonance there is no detuning i.e. $\delta = 0$, hence reflectivity is maximum. Under this situation of operating conditions, the reflectivity takes the form:

$$r_{max} \quad = \quad tanh^2(kL) \tag{20}$$

2.2 Properties of Fiber Bragg Grating

A lot of issues have to be taken into account when designing a reliable fiber Bragg grating. The more important one is the interference that may occur among the incident and the reflected waves along the optical fiber. Also, the coherence of the generated beams from the optical source is of primary concern. For the importance of these issues on the behavior of the FBG, this subsection is concerned with the discussion, briefly, of them. The coherence; the property that the light waves it contains are in phase with one another, constitutes one of the laser beam's unique properties. Coherence is important in applications such as holography and some types of spectroscopy and communication. For any electromagnetic wave, two types of coherence namely spatial and temporal coherence can be distinguished. Temporal coherence is the correlation between the fields at two different times (t_1, $t_2 = t_1 + \tau$) in the same wave train. This type of coherence is useful in interferometry because the formation of interference fringes is a manifestation of the temporal coherence between interfering beams,

since their ability to form fringes may be explained as arising from correlations that exist between them under conditions where a time delay has been introduced. Correlation functions are used to describe a laser beam's coherence properties. The degree of temporal coherence can be obtained from the measurement of the fringe visibility function. This function quantifies the contrast of interference in any system which has wave-like properties, such as optics, quantum mechanics, water waves, or electrical signals. Generally, two or more waves are combined and as the phase between them is changed, the power or intensity of the resulting wave oscillates forming an interference pattern. The ratio of the size or amplitude of these oscillations to the sum of the powers of the individual waves is defined as the visibility. Visibility is a quantitative measurement of the coherence of a light source. The fringe visibility will have a value between 0 and 1. The maximum visibility will occur when the two waves have equal intensity. The visibility will drop to zero when one of the waves has zero intensity. In general, the intensities of the two waves can vary with position, so that the average intensity and fringe visibility can also vary across the fringe pattern. The average intensity in the observation plane equals the sum of the individual intensities of the two interfering waves. The interference term redistributes this energy into bright and dark fringes. This is the role that the fringe visibility can play in formulating the fringe pattern.

Here, we have investigated two, weak and strong, different types of fiber Bragg gratings. The effect of their different parameters, including the fringe visibility, on their reflectivity, spectral bandwidth and maximum wavelength is analytically studied. The wavelength at which maximum reflectivity occurs has a mathematical form given by [9]:

$$\lambda_{max} = \left(1 + \frac{\overline{\delta n_{eff}}}{n_{eff}} \right) \lambda_D \qquad (21)$$

It is evident that the maximum wavelength drifts from design wavelength by a factor of $\frac{\overline{\delta n_{eff}}}{n_{eff}} \lambda_D$. This increase in the peak wavelength is useful for experimentally determining the induced index change while photo-writing the grating. On the other hand, the normalized bandwidth between the first zeros of the grating can be mathematically formulated as [12]:

$$\frac{\Delta \lambda_0}{\lambda_D} = v \frac{\overline{\delta n_{eff}}}{n_{eff}} \sqrt{1 + \left(\frac{\lambda_D}{v \overline{\delta n_{eff}} L} \right)^2} \qquad (22)$$

The weak grating is characterized by very small value of "kL" so the normalized bandwidth of that type of grating can be approximated to become:

$$\frac{\Delta \lambda_0}{\lambda_D} \cong \frac{2}{N} \quad \& \quad N \triangleq \frac{L}{\Lambda} \qquad (23)$$

Where N is the number of periods within the grating of length L. For strong gratings, on the other hand, "kL" is large and the normalized bandwidth can be simplified to:

$$\frac{\Delta \lambda_0}{\lambda_D} \cong v \frac{\overline{\delta n_{eff}}}{n_{eff}} \qquad (24)$$

As can be seen from the previous formulas, the normalized bandwidth for weak fiber Bragg grating is dependent only on the grating length whilst in the case of strong fiber Bragg grating, it depends mainly on the refractive index modulation and is independent of the grating length [13].

2.3 Photosensitivity and Fabrication Techniques

Photosensitivity means the periodic perturbation of the refractive index along the core of the fiber. This property makes it available for the fabrication of fiber Bragg grating across the core of the optical fiber. The first technique used for the fabrication of fiber Bragg grating depends on the use of continuous wave blue light from an Argon ion laser which has a wavelength of 488 nm [6]. This light wave was launched into a short segment of mono-mode optical fiber and then the intensity of the reflected light was monitored. At first, the intensity of the reflected light was low then after a period of few minutes, it grows in strength until almost all the light launched into the fiber is back-reflected. This growth in the reflected light was due to the effect of photosensitivity of optical fiber which enables an index grating to be written in the fiber. This increase in the reflected light intensity comes from the fact that coherent light propagating in the fiber interferes with a small amount of light reflected back from the end of the fiber to set a standing wave pattern which through photosensitivity writes an index grating in the core of the fiber. As the strength of the grating increases the intensity of the reflected light is
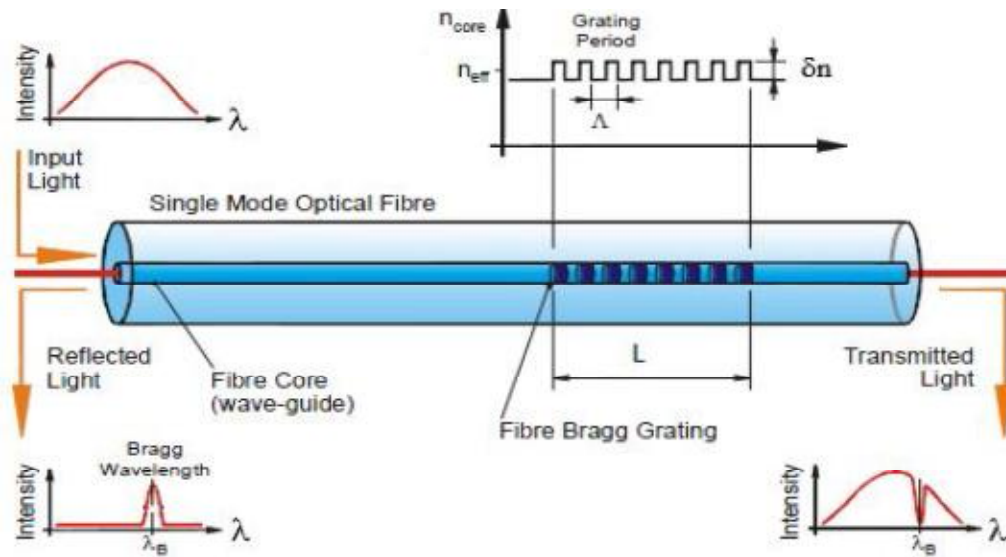
Fig. 1. Fiber Bragg grating structure

increased until it reaches saturation. 90% reflectivity is achieved with the use of Argon-ion laser experiment. The disadvantage of this type of grating (Hill gratings) was that it works only at wavelengths near the writing wavelength [7]. This limitation was overcome about ten years later in an experiment by Meltz et al. In his experiment, he used ultraviolet light with wavelength of 244 nm. The fiber is irradiated from the side with two intersecting coherent ultraviolet light beams. The two overlapping ultraviolet light beams interfere with each other producing a periodic interference pattern that writes the corresponding periodic index grating in the core of the fiber. This technique was called the transverse holographic technique. This technical processing has the advantage that the cladding is transparent to ultraviolet light but the core is highly absorbing to the ultraviolet light. So, this technique has the advantage of the ability of forming Bragg grating in the fiber core without removing the glass cladding. This process of fabrication has also another advantage which is: the Bragg grating could be made to work at much longer wavelengths in a spectral region of interest. This is because the period of the photo-induced grating depends on the angle between the two interfering coherent ultraviolet light beams, as Fig. 1 illustrates the basic structure of such technique of grating.

3. NUMERICAL SIMULATION RESULTS

The reflectance spectra of the reflection FBGs were MATLAB simulated according to the theoretical background that is previously outlined. The simulation is based on the solution of the coupled-mode equations. Our object here is to elucidate the effect of some parameters on the spectral response of two types of gratings: weak fiber Bragg grating (WFBG) and strong fiber Bragg grating (SFBG). These parameters include the fringe visibility, the grating period, the grating length and the refractive index modulation. Their effects on the reflectivity, spectral bandwidth, and maximum wavelength are examined. The parameters used in this simulation are chosen to be as follows: the designed wavelength is $\lambda_D = 1550nm$, the effective refractive index $n_{eff} = 1.45$, the fringe visibility is allowed to be varied in the range $0.7 \leq v \leq 1.0$. For WFBG, in which the refractive index modulation is small, we have taken $\overline{\delta n_{eff}} = 8 \times 10^{-5}$, whilst it was chosen to be as $\overline{\delta n_{eff}} = 4 \times 10^{-4}$ for SFBG. The grating length is assumed to be $L = 1cm$ for both cases of gratings.

As a first point, the spectral response dependence of the fringe visibility parameter is investigated. Fig. 2 shows the effect of the fringe visibility "v" on the spectral response for weak fiber Bragg grating. It is obvious from the results of this plot that the fringe visibility has a significant effect on the maximum reflectivity of WFBG. As the fringe visibility increases, the maximum reflectivity as well as the spectral bandwidth is increased. However, there is a slight shift, towards larger wavelengths, for the

maximum wavelength due to the increased value of the underlined parameter. Note that the maximal reflectivity does not occur at the designed wavelength "λ_D". This is because $\lambda_D =$ $2n\Lambda$ is valid for Bragg scattering by infinitesimally weak grating with a period Λ, which can be obtained as δn_{eff} approaches zero. In reality, the Bragg wavelength of grating is typically greater than the designed wavelength, for δn_{eff} larger than 0. Additionally, the obtained results demonstrate that as v acquires higher values, the side lobes are increased and the appearance of these secondary lobes is undesired for some practical applications of FBGs. This problem can be solved by using an apodization technique which depends on making the grading of the refractive index of the core to approach zero at its ends. This process provides a significant improvement in side lobes suppression without affecting the reflectivity or the bandwidth of FBG. Table 1 offers some numerical values of the underlined parameters to illustrate the role that they can play in controlling the characteristics of WFBG. Fig. 3 repeats the same thing for the SFBG under the same parameter values. The examination of the curves of this figure shows that the variation of the parameter of fringe visibility has no effect on the maximum reflectivity of SFBG on the contrary of WFBG. In general, strong gratings become saturated, and their reflectivity spectra exhibit flat top. Therefore, using saturated gratings will help us in achieving the desired square shape of the reflectivity spectrum. On the other hand, the change of v will affect both the spectral bandwidth and maximum wavelength. As Table 2 demonstrates, by giving v smaller or greater values, the reflection bandwidth can be made narrower or broader, respectively. In other words, the parameter v plays an important role in the width of reflection bandwidth of SFBG than in the case of WFBG. Additionally, it is noted that the maximum wavelength is shifted towards higher values as the value of v augments similar to the case of WFBG.
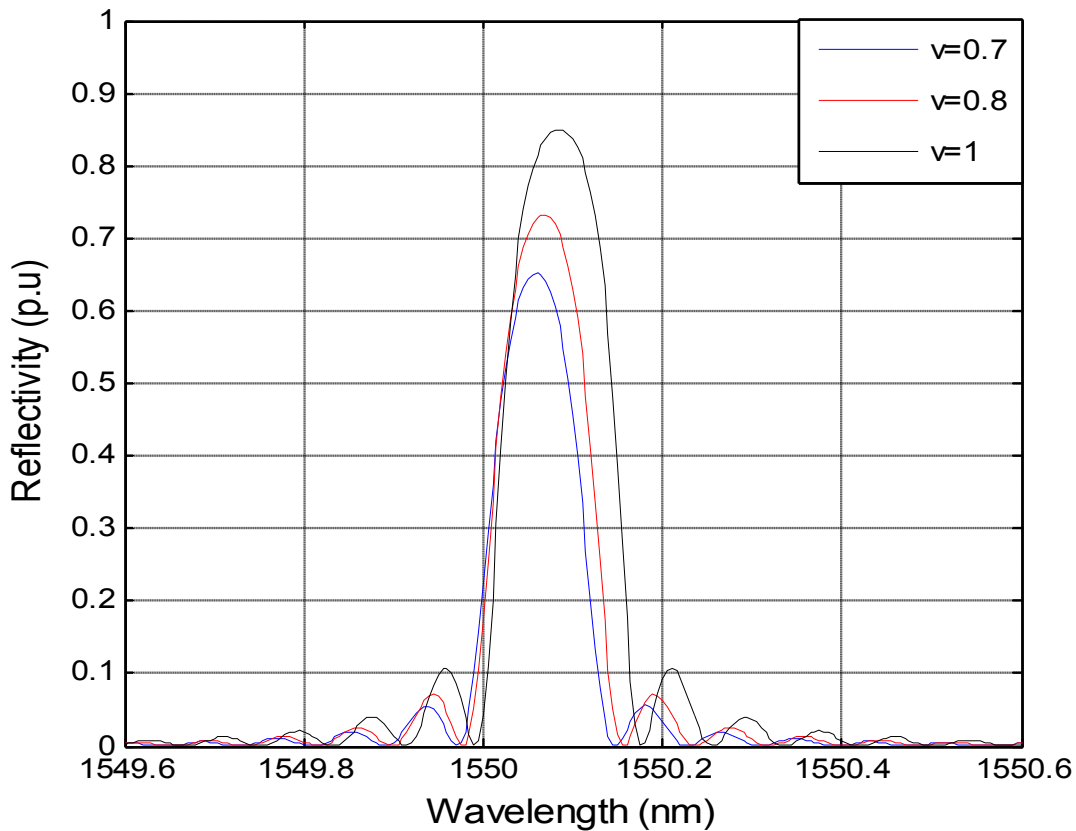

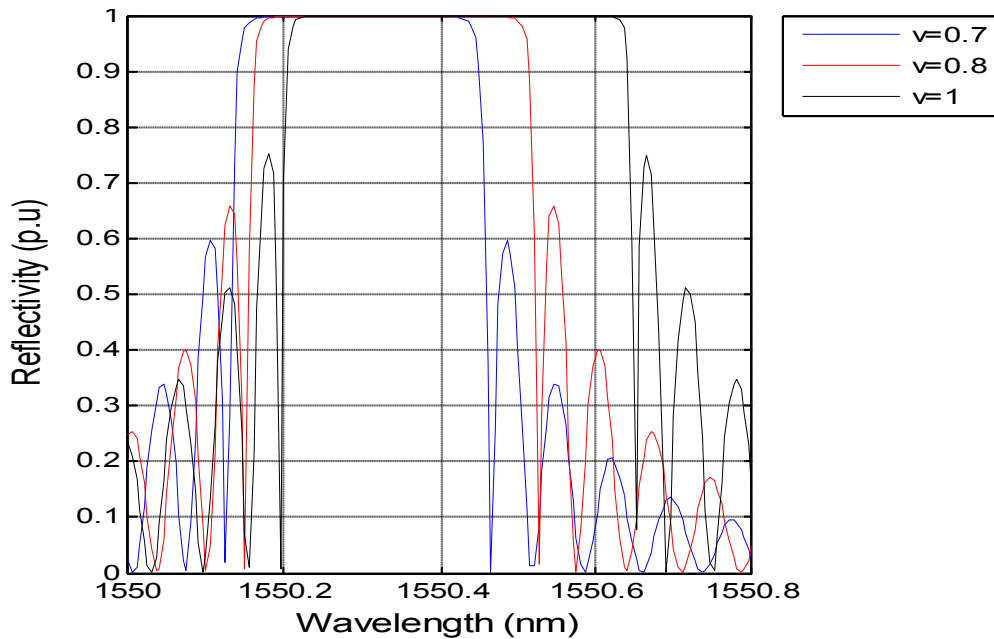**Fig. 2. Effect of fringe visibility on the spectral response of WFBG**

Fig. 3. Effect of fringe visibility on the spectral response of SFBG

Table 1. Effect of fringe visibility on the spectral response of WFBG

Fringe visibility	$v_1 = 0.7$	$v_2 = 0.8$	$v_3 = 1$
Maximum reflectivity (p.u)	0.650497	0.733041	0.848451
Maximum wavelength (nm)	1550.055	1550.07	1550.08
Normalized bandwidth	$1.1365*10^{-4}$	$1.1565*10^{-4}$	$1.2*10^{-4}$

Table 2. Effect of fringe visibility on the spectral response of SFBG

Fringe visibility	$v_1 = 0.7$	$v_2 = 0.8$	$v_3 = 1$
Maximum reflectivity (p.u)	1	1	1
Maximum wavelength (nm)	1550.427	1550.427	1550.427
Normalized bandwidth	0.000193	0.000221	0.000276

Table 3. Effect of grating period on the spectral response of WFBG

Grating period (nm)	$\Lambda_1 = 534.4\ 0$	$\Lambda_2 = 534.4\ 8$	$\Lambda_1 = 534.6\ 0$
Maximum reflectivity (p.u)	0.8553	0.8551	0.8551
Maximum wavelength (nm)	1549.845	1550.075	1550.425

Table 4. Effect of grating period on the spectral response of SFBG

Grating period (nm)	$\Lambda_1 = 534.4\ 5$	$\Lambda_2 = 534.4\ 8$	$\Lambda_1 = 534.50$
Maximum wavelength (nm)	1550.33256	1550.4195	1550.4776

Table 5. Effect of refractive index modulation on the spectral response of WFBG

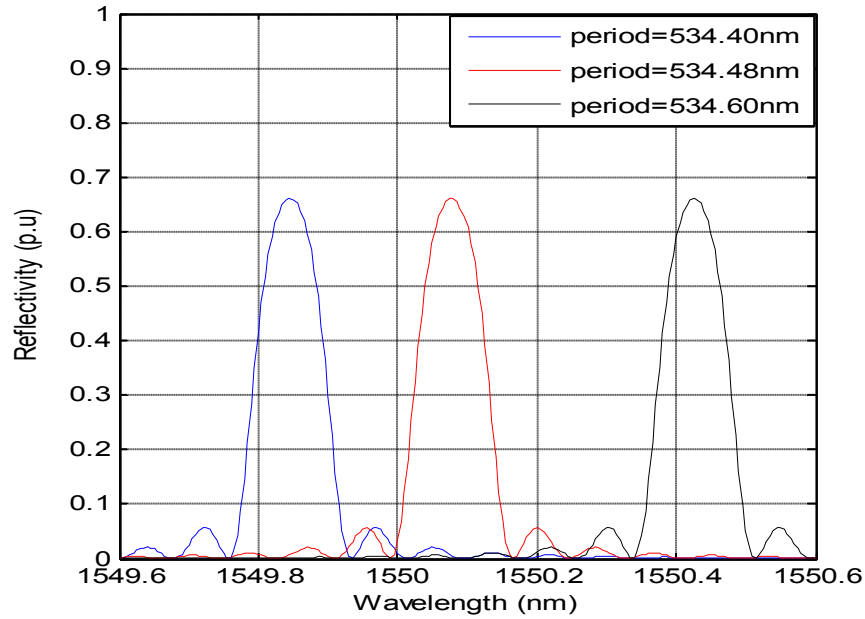| Refractive index modulation	$\overline{\delta n_{eff}} = 6*10^{-5}$	$\overline{\delta n_{eff}} = 6*10^{-5}$	$\overline{\delta n_{eff}} = 6*10^{-5}$
Maximum reflectivity (p.u)	0.6939	0.849453	0.929343
Maximum wavelength (nm)	1550.06	1550.085	1550.1
Normalized bandwidth	$1.146*10^{-4}$	$1.2*10^{-4}$	$1.272*10^{-4}$

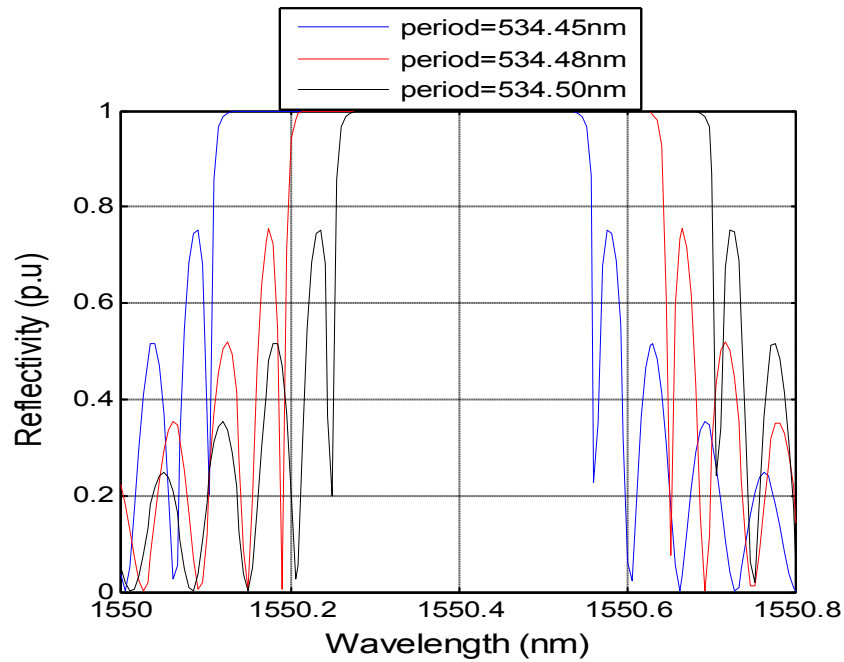**Fig. 4. Effect of grating period on the spectral response of WFBG**

Fig. 5. Effect of grating period on the spectral response of SFBG

Table 6. Effect of refractive index modulation on the spectral response of SFBG

Refractive index modulation	$\overline{\delta n_{eff}} = 6 * 10^{-5}$	$\overline{\delta n_{eff}} = 6 * 10^{-5}$	$\overline{\delta n_{eff}} = 6 * 10^{-5}$
Maximum wavelength (nm)	1550.32	1550.42	1550.481
Normalized bandwidth	0.000206	0.000277	0.000311
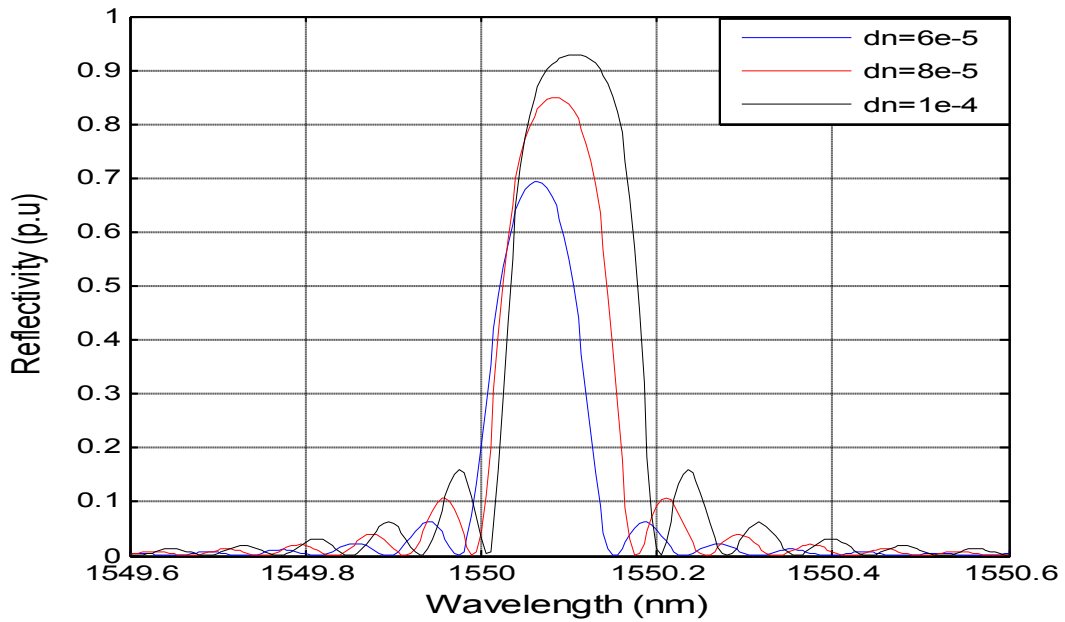
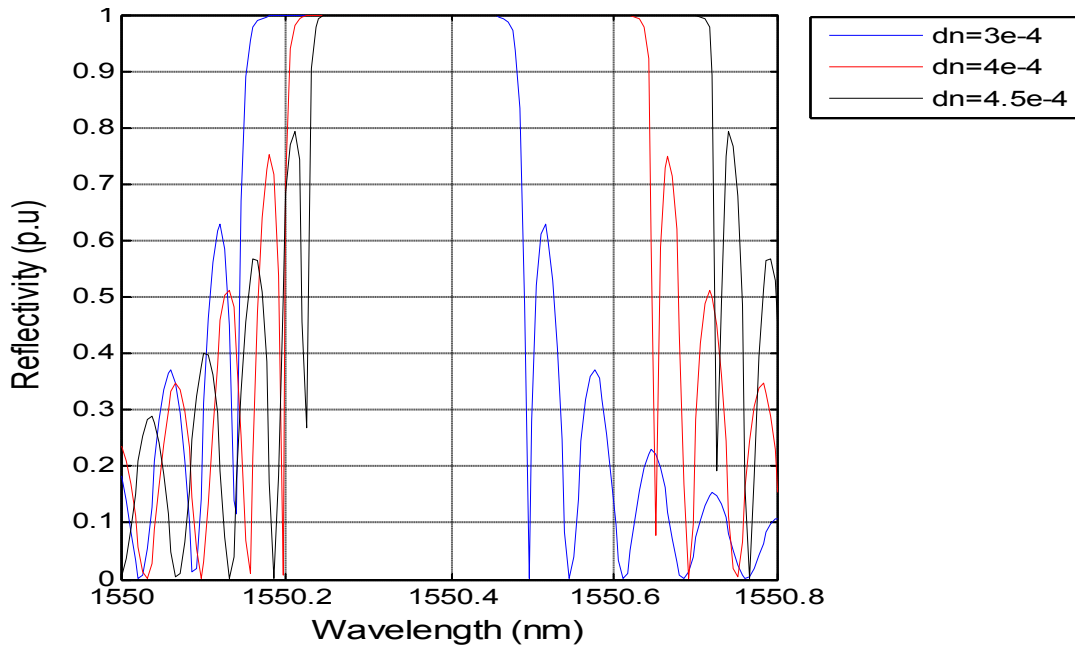**Fig. 6. Effect of refractive index modulation on WFBG**

Fig. 7. Effect of refractive index modulation on the spectral response of SFBG

Table 7. Effect of grating length on the spectral response of WFBG

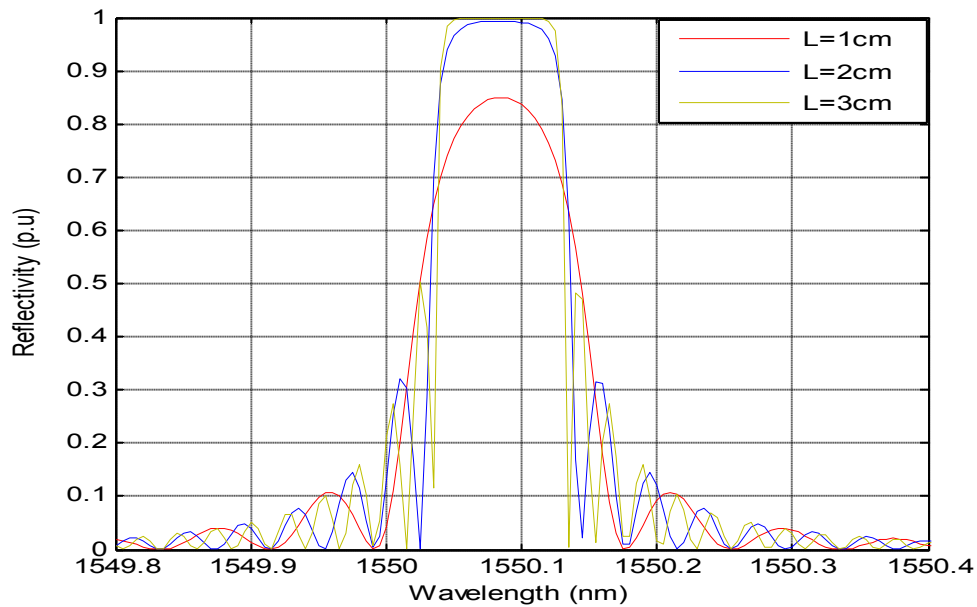| Grating length (cm)	$L_1 = 1$	$L_1 = 2$	$L_1 = 3$
Maximum reflectivity (p.u)	0.929	0.99	1
Maximum wavelength (nm)	1550.085	1550.085	1550.085
Normalized bandwidth	0.000225	0.000112	0.000075

Fig. 8. Effect of grating length on the spectral response of WFBG
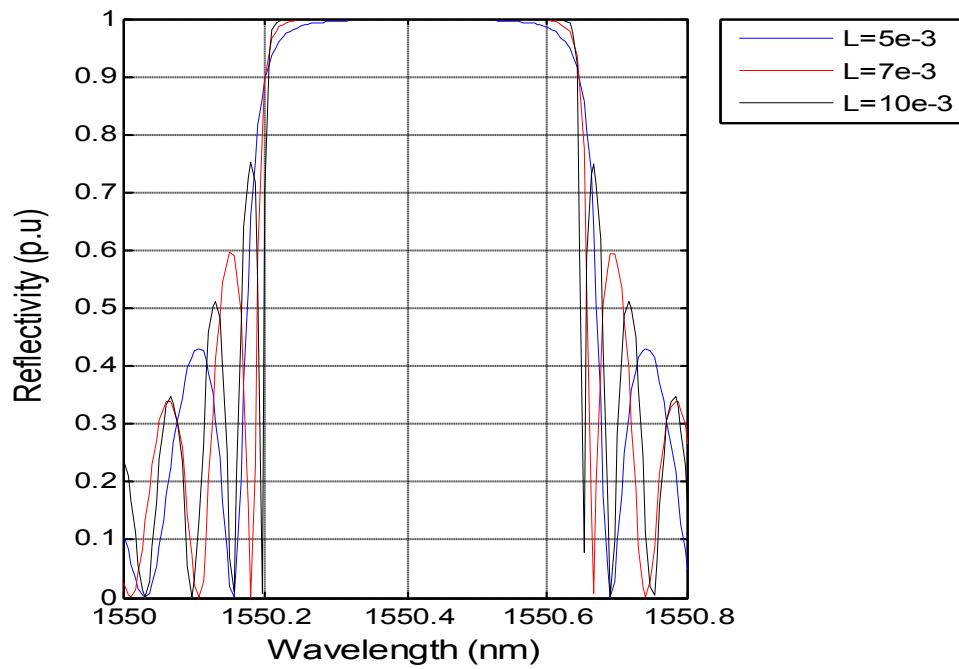

Fig. 9. Effect of grating length on the spectral response of SFBG

Table 8. Effect of grating length on the spectral response of SFBG

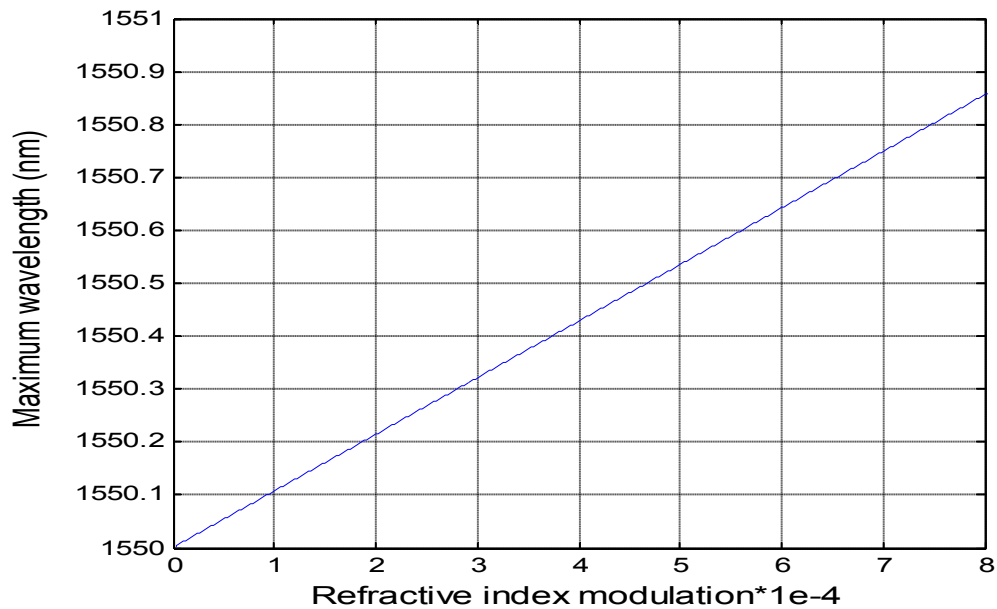| Grating length (mm)	$L_1 = 5$	$L_1 = 7$	$L_1 = 10$
Maximum reflectivity (p.u)	1	1	1
Maximum wavelength (nm)	1550. 427	1550.427	1550.427
Normalized bandwidth	$3.49*10^{-4}$	$3.15*10^{-4}$	$3*10^{-4}$

13

Fig. 10. Relation between refractive index modulation and maximum wavelength
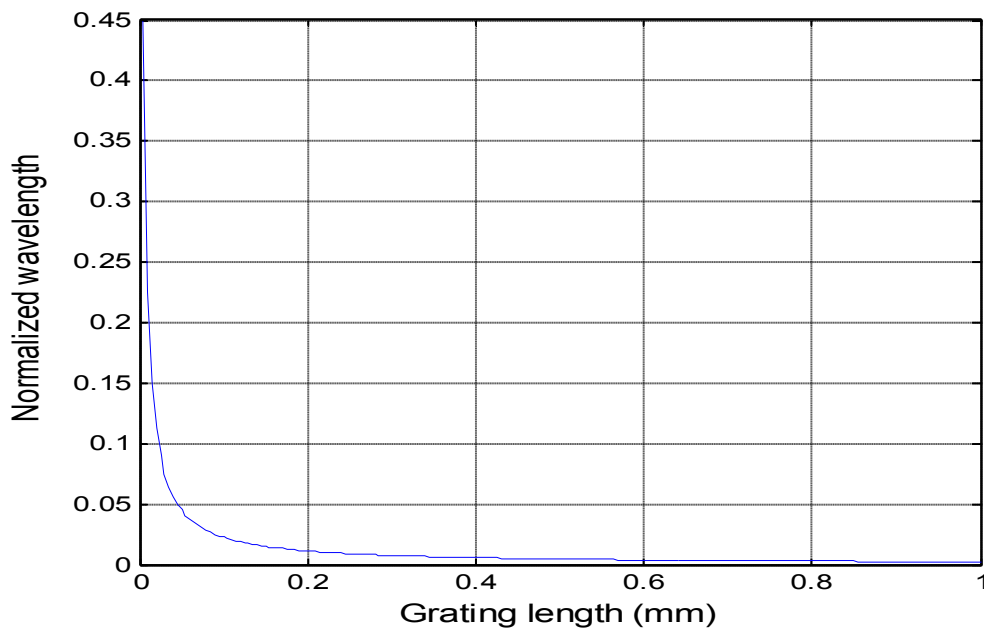

Fig. 11. Relation between normalized bandwidth and grating length for WFBG

Let us turn our attention to the effect of the grating period on the spectral response of the underlined FBGs. Fig. 4 displays the WFBG's reflectivity as a function of the operating wavelength for several grating periods. The family of curves of this scene clearly exhibits that the grating period has a significant impact on the reflectivity of the fiber Bragg grating especially the operating wavelength that catches maximum reflectivity "λ_{max}". It is observed that λ_{max} moves towards longer values by extending the grating period. Additionally, there is a noticeable shift of maximum wavelength as the grating period changes. Moreover, the variation of the grating period does not nearly affect the level of maximum reflectivity in contrast to the variation

of the parameter of fringe visibility where the level of maximum reflectivity increases with its increasing, as Fig. 2 demonstrates. Furthermore, the spectral bandwidth of WFBG rests approximately unchanged whether the grating period increases or not. Generally, as the grating period is increased, there is a little decrease in the maximum reflectivity and a little increase in the spectral bandwidth in the case of weak FBG. Some numerical values for the interesting parameters are depicted in Table 3. Fig. 5 represents a replica version of Fig. 4 for the same parameter values in the case of strong FBG. It was observed that, like the WFBG, the changing of the grating period affects only the maximum wavelength and does not have any effect neither on the maximum reflectivity nor on the spectral bandwidth. On the other hand, the variation of the grating period gives the same level of maximum reflectivity, which attains its full scale, as the variation of the fringe visibility in the case of strong FBG. Additionally, the existence of the side lobes in the performance of SFBG is more intense than in the case of WFBG under the behavior of the two indicated parameters. Table 4 gives the reader an idea about the effect of the changing of the under investigation parameters on the behavior of the SFBG.

The next category of curves is concerned with studying the impact of refractive index modulation on the spectral response of the two types of FBG under investigation. The family of this group includes Figs. 6-7: one plot for each type. For WFBG, see Fig. 6, there is an increase in the level of maximum reflectivity with the increasing of the refractive index modulation. It has a little effect on the spectral bandwidth and maximum wavelength. The spectral bandwidth, on the other hand, varies with the changing of the underlined parameter in such a way that it increases with its increasing and vice versa. The number of side lobes also increases as the refractive index modulation increases. For illustrating the range of values of the considered parameters, Table 5 is devoted to represent this purpose. In Fig. 7, the effect of refractive index modulation was investigated for the SFBG. It was noticed that the change in the refractive index modulation has a significant effect on the spectral bandwidth and maximum wavelength. Besides, it does not affect the maximum reflectivity as the previously mentioned parameters. As in the case of WFBG, the spectral bandwidth depends on the operating value of the refractive index modulation. The
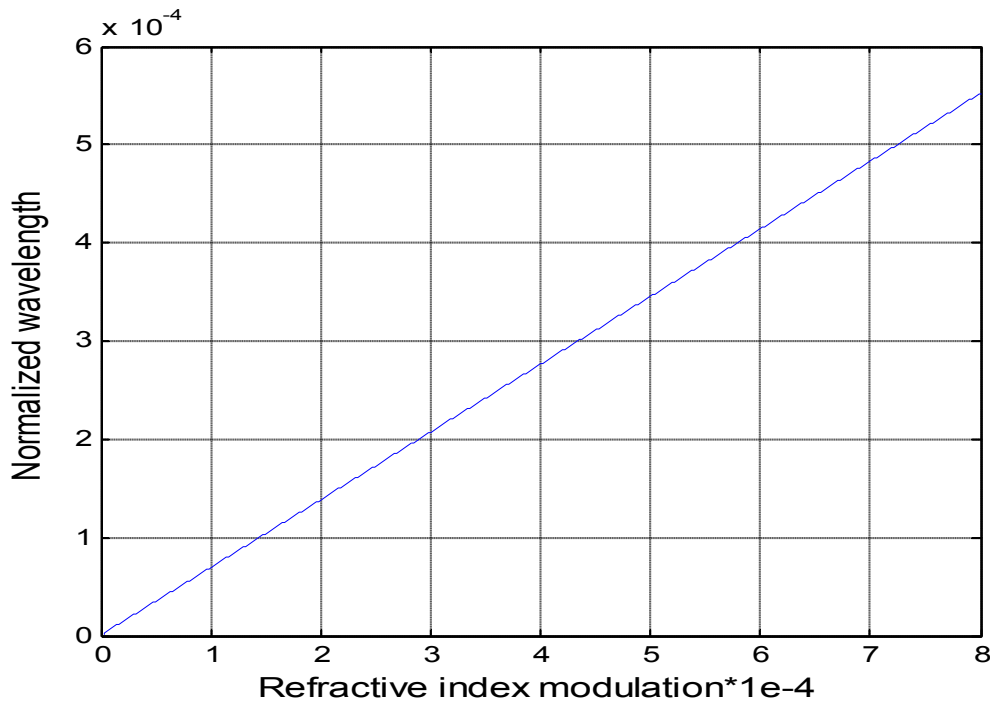

Fig. 12. Normalized bandwidth as a function of the refractive index modulation for SFBG

15

central wave length of maximum reflectivity is shifted towards longer values as the modulation of the refractive index becomes condensed. Some of our numerical results are displayed in Table 6 to explain to what extent the grating parameters can vary its performance.

Finally, the influence of the grating length on the behavior of the under examined FBGs is tested in Figs. 8-9. Fig. 8 illustrates that the grating length of WFBG does not have any effect on the maximum wavelength which means that λ_{max} remains unchanged with the changing of the concerned parameter. As Table 7 demonstrates, the grating length plays a noticeable role on the level of maximum reflectivity where it is increased as the underlined parameter increases. The spectral bandwidth, on the other hand, decreases with the increasing of the grating length. The side lobes follow also the variation of the grating length where they are increased by its increasing. Fig. 9 depicts the same thing for the SFBG. The spectral bandwidth of strong fiber Bragg grating is independent of the grating length as the light does not penetrate the full length. The change in the grating length does not affect the maximum wavelength as well. The only effect that the grating length produces in the SFBG is that as it is increased, the spectral response takes a square shape in its variation and becomes a more flat so the desired square shape of the reflectivity can be easily achieved. Table 8 exhibits some numerical values for the concerned parameters to show their role in controlling the characteristics of the FBG under consideration.

In order to clearly elucidate how can λ_{max} varies with the refractive index modulation, Fig. 10 is devoted to illustrate this variation. By examining the results of this scene, it is obvious that the maximum wavelength increases as the refractive index modulation increases in a linear fashion for both weak and strong FBGs. Fig. 11, on the other hand, shows the relation between normalized bandwidth and grating length for WFBG. It was clear that for WFBG, the normalized bandwidth is dependent on the grating length. As the grating length is increased, the normalized bandwidth is decreased. For strong FBG, the normalized bandwidth depends on the refractive index modulation. The relation between normalized bandwidth and refractive index modulation is shown in Fig. 12.

4. CONCLUSION

In this paper, two types of uniform Bragg gratings were simulated. The coupled-mode theory as a suitable tool of analysis is used to analyze them. Their spectra with different parameter values were simulated and discussed.

By varying some parameters such as fringe visibility, grating period, grating length and refractive index modulation, it is possible to obtain narrow-band transmission as well as high reflectivity at the Bragg wavelength. Optimization of these parameters is the main aim of any designer for achieving the maximum performance of the FBG in its practical uses and especially in band-pass filtering applications such as wavelength multiplexing/de-multiplexing and add/drop optical filter.

The results of our FBGs simulation elucidate that these parameters have a significant effect on the maximum reflectivity, spectral bandwidth and maximum wavelength of weak and strong fiber Bragg gratings. By adjusting the values of these parameters, we can obtain the desired spectral response with high reflectivity and narrow bandwidth. We have concluded that the maximum reflectivity of FBG is improved as the fringe visibility, grating length, or refractive index modulation increases. On the other hand, it is degraded as the grating period augments. Additionally, the spectral bandwidth of weak FBG is length limited while that of strong FBG depends upon the refractive index modulation. Moreover, there is a significant shift for maximum wavelength towards longer values when the grating period is elevated and this occurs for both weak and strong FBGs. Furthermore, the reflectivity attains always its full level (100%) at the design wavelength for strong FBG whilst it increases when the fringe visibility, refractive index modulation, or the grating length increases and vice versa in the case of weak FBG.

COMPETING INTERESTS

Authors have declared that no competing interests exist.

REFERENCES

1. Hill KO, Meltz G. Fiber Bragg Grating technology: fundamentals and overview. J Lightwave Technol. 1997;15:1263–1276.

2. Dinesh Arora, Jai Prakash, Hardeep Singh, Amit Wason. Reflectivity and braggs wavelength in FBG. International Journal of Engineering (IJE). 20115;341-349.
3. Abdallah Ikhlef, Rachida Hedara, Mohamed Chikh-bled. Uniform Fiber Bragg grating modelling and simulation used matrix transfer method. IJCSI international journal of computer science issues. 2012;9:368-374.
4. El Mashade MB, Nady M. BOR-FDTD analysis of nonlinear Fiber Bragg grating and distributed Bragg resonator. Optics & Laser Technology. 2011;43:1065–1072.
5. Jianfeng Zhao. An object oriented simulation program for fiber Bragg gratings. Master of Engineering, South Africa; 2001.
6. Shanglin Hou, Yunbo Shang, Yanjun Liu, Jingli Lei, Yongzhao Xu. Influence of grating period of uniform fiber bragg grating on slow light delay. Progress in Electromagnetics Research Symposium Proceedings, Suzhou, China. 2011;934-937.
7. Kashyap R. Fiber Bragg Gratings. San Diego: Academic press; 1999.
8. Santosh Pawar, Shubhada Kumbhaj, Pratima Sen, Pranay Kumar Sen. Fiber bragg grating filter for optical communication: Applications and Overview. International Journal of Advanced Electrical and Electronics Engineering, (IJAEEE). 2013;2(4):51-58.
9. Othonos A. Fiber Bragg gratings. Review of Scientific Instruments. 1997;68:4309-4341.
10. Jyotsna Rani Mahapatra, Manisha Chattopadhyay. Spectral characteristics of uniform fiber Bragg grating using coupled mode theory. International journal of Electrical, Electronics and Data communication. 2013;1:40-44.
11. Xiaofu Li, Haihu Yu, Hua Huang, Dongsheng Zhang. Numerical simulation and analysis of spectral characteristic for weak fiber Bragg grating. International Conference on Electronic & Mechanical Engineering and Information Technology. 2011;2435-2438.
12. Turan Erdogan T. Fiber grating spectra. Journal of Lightwave Technology. 1997; 15:1277-1294.
13. Tawfik NI. Eldeeb WS, El_Mashade MB, Abdelnaiem AE. Optimization of uniform fiber bragg grating reflection spectra for maximum reflectivity and narrow bandwidth. International Journal of Computational Engineering Research (IJCER). 2015;5(2):53-61.

Peer-review history:
The peer review history for this paper can be accessed here:
http://sciencedomain.org/review-history/10212